Modelling Simul. Mater. Sci. Eng. **12** (2004) 973–983 PII: S0965-0393(04)80990-2

Analysis of flow development in centrifugal atomization: Part II. Disintegration of a non-fully spreading melt

Y Y Zhao

Department of Engineering, The University of Liverpool, Brownlow Hill, Liverpool L69 3GH, UK

Received 11 November 2003
Published 9 August 2004
Online at stacks.iop.org/MSMSE/12/973
doi:10.1088/0965-0393/12/5/014

Abstract

Centrifugal atomization of metal melts is a cost-effective process for powder production and spray deposition. The properties of the as-produced powder and deposit are determined primarily by the characteristics of the atomized droplets, which in turn are largely dependent on the flow development of the melt on the atomizer. This paper develops a model for analysing the flow development of a non-fully spreading melt on the atomizing cup. The model shows that the melt can disintegrate prematurely before reaching the edge of the cup when the dynamic contact angle of the melt exceeds a critical contact angle. The critical contact angle is very small for a flat disc but increases markedly with increasing slope angle of a cup. The critical contact angle also increases with increasing melt flow rate and cup rotation speed. The model gives a good insight into the atomization mechanism and explains well the phenomena observed in centrifugal atomization, including the conditions of the occurrence of the three atomization modes and the existence of an optimum melt flow rate, cup radius, cup slope angle and cup rotation speed for achieving small droplet sizes.

Nomenclature

A	area of the segment cross section
a	overall acceleration due to body forces
a_r	radial component of centrifugal acceleration
$\vec{a}$	centrifugal acceleration (vector)
g	gravitational acceleration
H	film thickness of the melt on the cup
h	normal coordinate from the cup surface

h_m	normal coordinate at the middle of the segment
P	a constant
Q	melt volume flow rate
$\vec{r}$	radial coordinate (vector)
R	radius of curvature of the segment
R_o	initial radius of curvature of the segment
r	radial coordinate in the cylindrical system
r_o	cup radius
r_1	ligament formation radius
r_2	droplet formation radius
y	horizontal coordinate
$\vec{v}$	melt velocity relative to the cup (vector)
$\bar{v}_\theta$	mean azimuthal melt velocity relative to the cup
α	cup slope angle
φ	inclination angle of the segment
φ_c	critical dynamic contact angle
φ_o	dynamic contact angle of the melt
μ	viscosity of the melt
ρ	specific density of the melt
σ	surface tension of the melt
Ω	cup rotation speed (rps)
$\vec{\omega}$	cup rotation speed (vector)
ω	cup rotation speed (radian s^{-1})

1. Introduction

In centrifugal atomization for powder production and spray deposition, the flow development of the melt on the atomizer has a significant influence on the quality of the resultant powder and deposit. In part I of this series, an analytical model has been developed to describe the melt flow both on and off an atomizer, either a flat disc or a cup, for a fully spreading melt [1]. In many cases, however, the melt flow on the atomizer is found to have already disintegrated into ligaments and even droplets instead of being a fully spreading continuous film [2]. The predictions of the analytical models developed for fully spreading melts [1, 3, 4] are not always consistent with the experimental observations [2] in terms of the relationship between the processing condition and the droplet size distribution. It is well known that centrifugal atomization may occur in three different modes: direct droplet formation, ligament disintegration or film disintegration. Hinze and Milborn [5] have proposed an empirical equation for water-based liquids to describe the transition from one mode to another, but the disintegration mechanisms are not fully understood. There is a need to study the flow development when premature disintegration of the melt takes place on the atomizer.

The degree of spreading of a melt on the surface of a solid largely depends on the wettability of the solid by the melt, characterized by the contact angle, i.e. the angle of contact that the melt makes on the solid. The contact angle is determined by the interfacial tensions at the boundaries between the liquid, solid and atmosphere. For a molten metal, the wettability of a solid is dependent upon the nature of atomic bonding and the thermodynamic stability of the solid [6]. Ionic ceramics are relatively difficult to wet. Covalently bonded ceramics are more easily wetted by metals. Clean metals are usually well wetted by another metal.

The effective contact angle is also influenced by a large number of variables that include temperature, atmosphere, roughness, crystal structure, composition, surface pre-treatments, interfacial segregation, adsorption and reactions [6]. No solid–melt systems are practically fully wetting. Under dynamic conditions, the contact angle is also strongly dependent upon the local melt velocity and the pressure in the melt normal to the solid surface. It is often impractical to obtain a well-defined dynamic contact angle between a melt–solid couple. Nevertheless, examining the wettability between the melt and the atomizer as well as the flow dynamics can help understand how well the melt may spread on the atomizer. The degree of spreading can in turn help understand how the melt disintegrates.

This paper is to develop an analytical model for predicting the disintegration of a non-fully spreading melt on a rotating cup in centrifugal atomization. The model is not intended for accurate quantitative predictions because of the lack of reliable wettability information under dynamic conditions. Instead, the model is to provide a useful angle of view for understanding the atomization mechanism and how the variations in the processing parameters would affect the size distribution of the resultant droplets.

2. Model

The integrity of a melt flow on a rotating cup is related to the wettability of the cup by the melt. If the melt fully wets the cup, it spreads on the cup completely. The flow is axi-symmetric and has a circumferentially uniform film thickness, which can be calculated using the model developed in part I of this series [1]. If the melt does not fully wet the cup, it may or may not fully spread on the cup, subject to the outcome of two counteractions. On one hand, the surface tension of the melt tends to result in its retraction from the cup surface if it does not fully wet the cup. On the other hand, the gravitational and centrifugal forces press the melt towards the cup and enhance its spreading on the cup. If the latter is dominant, the melt remains a complete film. If the former becomes dominant, however, the film starts to disintegrate into ligaments, and even further into droplets, before reaching the edge of the cup.

Let us consider how the balance between the surface tension and the pressing forces would affect the evolution of the circumferential cross section of the flow on a rotating cup. If the melt spreads fully along the circumference, the circumferential cross section normal to the cup wall at radius r is a cylinder with a circumference of $2\pi r$ and a height of H [1]:

$$H = \left[\frac{3\mu Q}{2\pi\rho\omega^2 r^2 \cos\alpha}\right]^{1/3}, \tag{1}$$

where ρ is the specific density of the melt, μ the viscosity of the melt, Q the volume flow rate of the melt, α the slope angle of the cup wall and ω is the rotation speed of the cup (scalar, in radian s^{-1}).

When the retracting tendency caused by surface tension exceeds the spreading one caused by the gravitational and centrifugal forces, the melt starts to break up at a certain point on the circumference. Assuming that the melt starts to disintegrate into a single ligament at radius r, cutting the cross section at the breaking point and flattening it would result in a segment with a base width of $2\pi r$ instead of a rectangle. The segment cross section is not expected to be symmetric because of the existence of an azimuthal velocity component in the melt. The azimuthal velocity relative to the cup is zero at the melt–cup interface but increases with the normal distance from the cup wall. There is therefore a sideways velocity in the ligament, except at the base of the segment. From the viewpoint of wetting-controlled spreading, one half of the segment can be seen as advancing and the other retreating. The dynamic contact angles at the two endpoints of the segment are therefore different. To simplify the analysis,

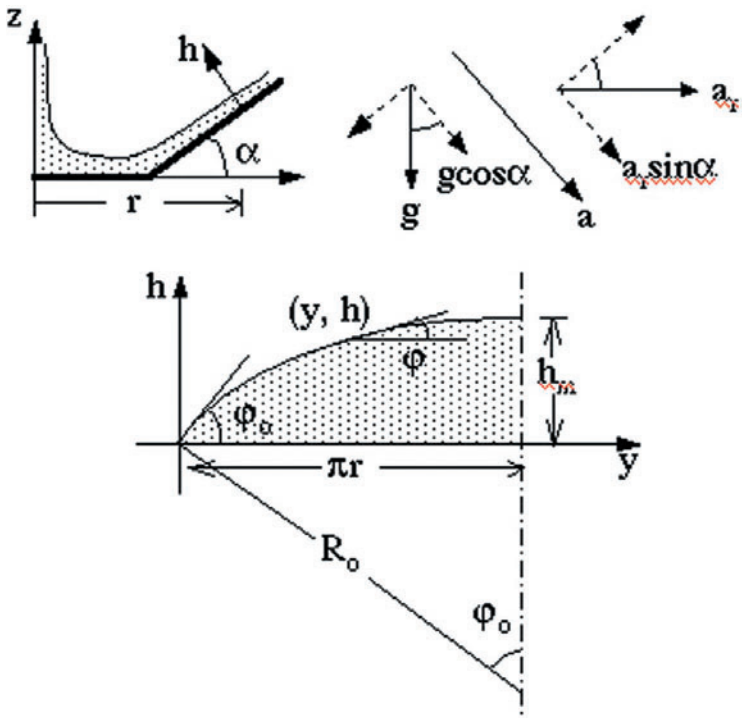

Figure 1. Schematic diagrams showing the gravitational and centrifugal accelerations in the melt normal to the cup wall and the cross section of a segment that might form due to partial wetting between the melt and the cup.

however, we can assume a symmetrical segment with the same base width and a representative dynamic contact angle. Since we are only concerned with the total area of the segment and not much with the exact value of the dynamic contact angle, the simplified approach should suffice.

Figure 1 shows schematically half of the segment when it first forms at a radius r, and the gravitational and centrifugal accelerations in the segment plane. The shape of the segment depends on the dynamic contact angle and the distribution of the gravitational and centrifugal forces in the liquid. To maintain a steady shape, the internal pressure must be the same everywhere in the segment. The sum of the pressures resulting from surface tension and body forces is therefore a constant along the top boundary of the segment:

$$\frac{2\sigma}{R} + \rho a(h_{\mathrm{m}} - h) = P, \tag{2}$$

where σ is the surface tension of the melt, R the radius of curvature of the top boundary at a point with a normal coordinate (i.e. the normal distance of the point to the base) of h, h_{m} the normal coordinate at the middle of the segment, a the overall acceleration in the normal direction to the base due to the body forces and P is a constant. The first and second terms on the left-hand-side of equation (1) are the internal pressures resulting from the surface tension [7] and the body forces, respectively.

Let us first consider the overall acceleration due to the body forces. The melt on the rotating cup is subject to gravitational and centrifugal forces, each of which has a component normal to the cup wall. The overall acceleration normal to the cup wall is the sum of the two corresponding acceleration components, as shown in figure 1, and can be expressed as

$$a = g\cos\alpha + a_r \sin\alpha, \tag{3}$$

where $g = 9.8\,\mathrm{m\,s^{-2}}$ is the gravitational acceleration and a_r is the radial component of the centrifugal acceleration.

The centrifugal acceleration on a small element of melt is [8]

$$\vec{a} = -[2\,\vec{\omega} \times \vec{v} + \vec{\omega} \times (\vec{\omega} \times \vec{r})], \tag{4}$$

where $\vec{\omega}$ is the rotation speed of the cup (vector), $\vec{v}$ is the velocity of the small element relative to the rotating cup (vector) and $\vec{r}$ is the radial coordinate of the element (vector). Assuming that the azimuthal slippage of the melt on the rotating cup is not significant, the azimuthal velocity of the melt can be treated as constant along the normal direction and can be represented by a mean value given by the analytical model in part I [1]. The radial component of the centrifugal acceleration can therefore be expressed as

$$a_r = \omega(\omega r + \bar{v}_\theta) = \omega^2 r \left\{ 1 - \frac{3}{5}\left[\frac{2\rho Q^2\cos\alpha}{3\pi^2\mu\omega r^4}\right]^{2/3} \right\}, \tag{5}$$

where $\bar{v}_\theta$ is the mean azimuthal velocity of the melt relative to the cup [1].

Let us now consider the variation of the radius of curvature of the segment. For the ligament on the cup to be in the equilibrium state, the inclination angle of the top boundary of the segment (i.e. the angle between the tangent of the top boundary and the base of the segment) at the breaking point ($h = 0$) must be equal to the dynamic contact angle of the liquid, φ_o. The radius of curvature at the breaking point, R_o, can be treated as equal to the radius of a circular arc, the chord of which is equal to the base of the segment in length and the initial inclination angle of which is equal to the dynamic contact angle, φ_o. The initial radius of curvature at $h = 0$ is therefore $R_o = \pi r/\sin\varphi_o$, as illustrated in figure 1. The reciprocal of the radius of curvature is termed as curvature. Taking this initial condition into account, the curvature of the top boundary of the segment at any point with a normal coordinate of h can be derived from equation (2) as

$$\frac{1}{R} = \frac{\sin\varphi_o}{\pi r} + \frac{\rho}{2\sigma} a h. \tag{6}$$

The curvature of a curve at a point is defined as the ratio of an infinitesimal change in the inclination angle to the corresponding infinitesimal change in the length of the curve at the given point. The curvature of the segment at any point can therefore be related to the changes in the inclination angle and normal coordinate of the top boundary at the given point by

$$\frac{1}{R} = -\frac{\sin\varphi\,\mathrm{d}\varphi}{\mathrm{d}h}, \tag{7}$$

where φ is the inclination angle of the top boundary of the segment at a point with a normal coordinate of h. Substituting equation (7) into equation (6) gives the differential relationship between φ and h as

$$-\sin\varphi\,\mathrm{d}\varphi = \left(\frac{\rho}{2\sigma} a h + \frac{\sin\varphi_o}{\pi r}\right)\mathrm{d}h. \tag{8}$$

Given the initial condition that $\varphi = \varphi_o$ at $h = 0$, integrating equation (7) gives the relationship between the inclination angle and the normal coordinate of the segment as

$$\cos\varphi = \cos\varphi_o + \frac{\sin\varphi_o}{\pi r} h + \frac{\rho}{4\sigma} a h^2. \tag{9}$$

At the middle of the segment, the inclination angle $\varphi = 0$ and the corresponding normal coordinate is therefore

$$h_{\mathrm{m}} = \frac{2\sigma}{\rho a}\left[\sqrt{\left(\frac{\sin\varphi_{\mathrm{o}}}{\pi r}\right)^2 + \frac{\rho a}{\sigma}(1-\cos\varphi_{\mathrm{o}})} - \frac{\sin\varphi_{\mathrm{o}}}{\pi r}\right]. \tag{10}$$

As the changes in the horizontal and normal coordinates of the segment (y, h) follow the relation $\mathrm{d}y = ctg\varphi\,\mathrm{d}h$, the area of the segment can be calculated using

$$A = 2\int_0^{\pi r} h\,\mathrm{d}y = 2\int_0^{h_{\mathrm{m}}} h\,ctg\varphi\,\mathrm{d}h. \tag{11}$$

To satisfy the mass conservation criterion, this area must be equal to the cross-sectional area of the melt film just before the disintegration takes place, i.e. $A = 2\pi r H$. Combining equations (1) and (11) gives

$$\int_0^{h_{\mathrm{m}}} h\,ctg\varphi\,\mathrm{d}h = \left[\frac{3\pi^2\mu Q r}{2\rho\omega^2\cos\alpha}\right]^{1/3}. \tag{12}$$

Given ρ, μ, σ, Q, ω, α and φ_{o}, r becomes the only unknown parameter in equation (12) and can be determined. The radius that satisfies equation (12) is the radius at which the uniform melt film on the cup starts to disintegrate into ligaments and is designated as the ligament formation radius, r_{c1}. Equation (12) can also be used to determine the operating condition under which the ligament formation radius coincides with the cup radius, r_{o}. The analytical solution of equation (12) is too complex. It is much more convenient to solve it by numerical means.

3. Illustrations and discussions

To illustrate the model predictions, liquid tin has been used as a model melt. The physical properties used in the calculations are specific density $\rho = 6970\,\mathrm{kg\,m^{-3}}$, viscosity $\mu = 0.001\,97\,\mathrm{kg\,m^{-1}\,s^{-1}}$ and surface tension $\sigma = 0.57\,\mathrm{N\,m^{-1}}$ [9]. The operating parameters of the centrifugal atomization process are varied in the following ranges: volume flow rate, Q, 2.5×10^{-6}–$2\times10^{-5}\,\mathrm{m^3\,s^{-1}}$; cup rotation speed, Ω, 50–1000 rps (revolutions per second); and cup slope angle, α, 0–75°. A MATLAB programme has been created to solve equation (12) at a given set of conditions. It should be noted that for convenience the cup rotation speed shown in the illustrations is Ω, with a unit of rps. In the calculations, however, $\omega = 2\pi\Omega$, with a unit of radian $\mathrm{s^{-1}}$, being used instead.

Figure 2 shows the variations of the ligament formation radius, r_{c1}, with the dynamic contact angle, φ_{o}, for a series of cup slope angles, α, at a fixed volume flow rate $Q = 1\times10^{-5}\,\mathrm{m^3\,s^{-1}}$ and a fixed cup rotation speed $\Omega = 250$ rps. The ligament formation radius is extremely sensitive to the dynamic contact angle within a narrow range largely determined by the cup slope angle. For a fixed volume flow rate, cup rotation speed and cup slope angle, there exists a critical contact angle, φ_{c}, at which the ligament formation radius coincides with the cup radius ($r_{\mathrm{c1}} = r_{\mathrm{o}}$). If the dynamic contact angle of the melt is smaller than the critical value ($\varphi_{\mathrm{o}} < \varphi_{\mathrm{c}}$), the melt will remain a continuous film before reaching the edge of the cup. If the dynamic contact angle of the melt is greater than the critical value ($\varphi_{\mathrm{o}} > \varphi_{\mathrm{c}}$), however, the melt will have disintegrated before reaching the edge of the cup. The melt at the edge of the cup will be in the form of ligaments or even droplets. A convenient approach for examining the effects of the operating parameters of the centrifugal atomization process on the melt disintegration is therefore to examine their effects on the critical contact angle.

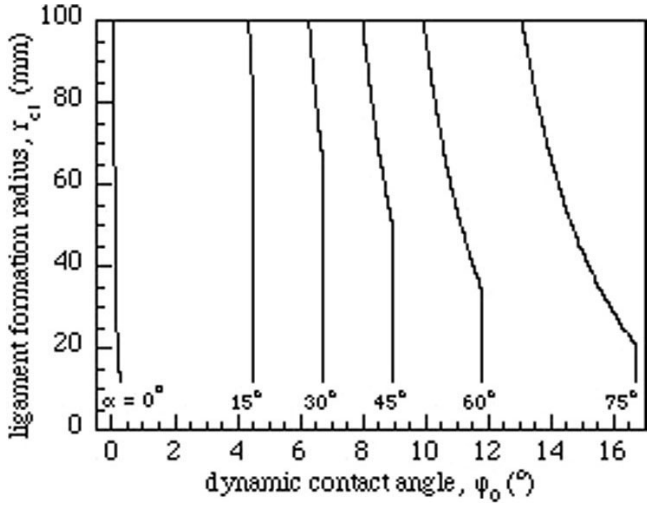

Figure 2. Variations of ligament formation radius, r_{c1}, with dynamic contact angle, φ_o, at different cup slope angles, α, at $Q = 1 \times 10^{-5}\,\mathrm{m^3\,s^{-1}}$ and $\Omega = 250$ rps.

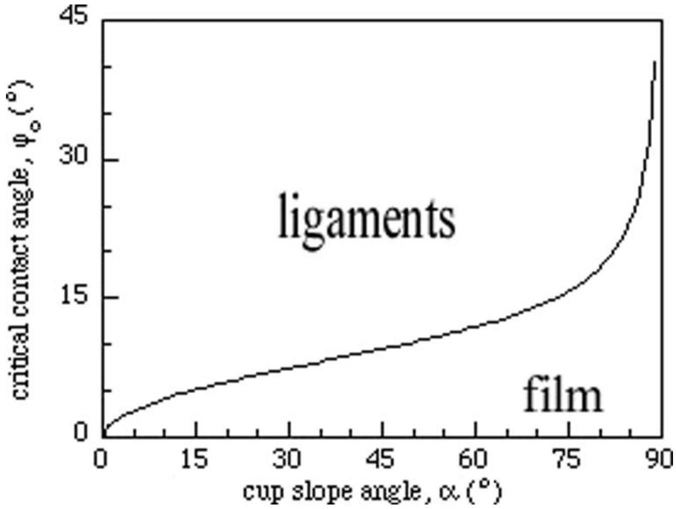

Figure 3. Variation of critical contact angle, φ_c, with cup slope angle, α, at $r_o = 0.03$ m, $Q = 1 \times 10^{-5}\,\mathrm{m^3\,s^{-1}}$ and $\Omega = 250$ rps.

Figures 3, 4 and 5 show the variations in the critical contact angle, φ_c, with the cup slope angle, α, volume flow rate, Q, and cup rotation speed, Ω, respectively. If not specified, the parameters other than the one in consideration are fixed as follows: cup radius $r_o = 0.03$ m, volume flow rate $Q = 1 \times 10^{-5}\,\mathrm{m^3\,s^{-1}}$ and cup rotation speed $\Omega = 250$ rps. For a flat disc ($\alpha = 0$), the critical contact angle increases with increasing melt flow rate and decreasing cup rotation speed. However, it is very small in any case and ranges from 0.05° to 0.26° in the wide range of conditions considered in this paper. Using a cup can increase the critical contact angle markedly, as shown in figure 3. For a cup ($\alpha \geqslant 15°$), the critical contact angle increases with increasing melt flow rate and cup rotation speed.

Numerical calculation of the ligament formation radius is only possible if the dynamic contact angle of the melt is known. However, it is very difficult to obtain a reasonably accurate

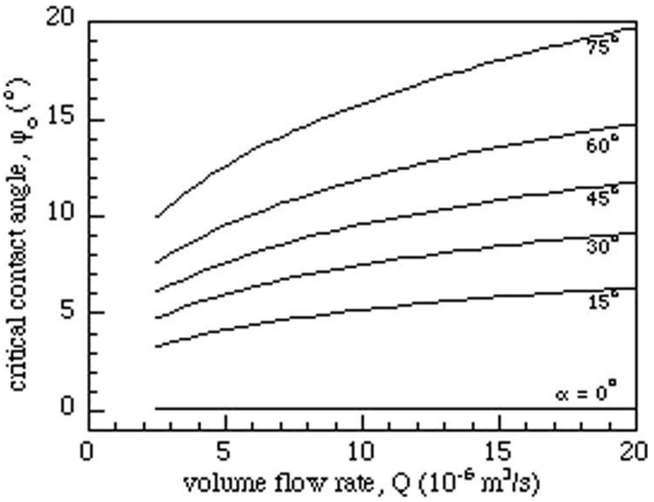

Figure 4. Variation of critical contact angle, φ_c, with melt volume flow rate, Q, at $r_o = 0.03$ m and $\Omega = 250$ rps.

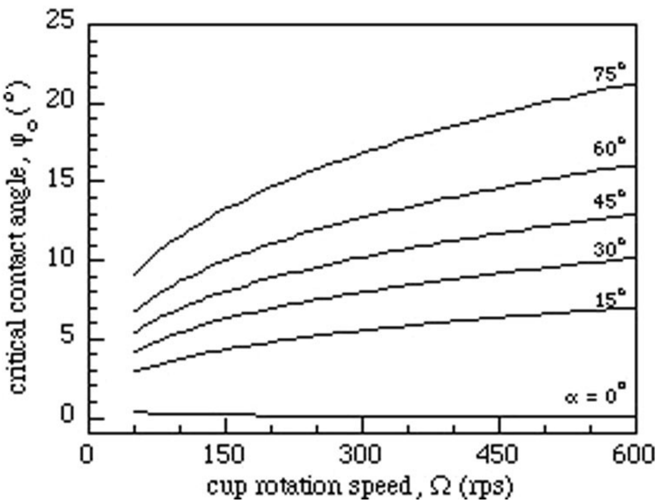

Figure 5. Variation of critical contact angle, φ_c, with cup rotation speed, Ω, at $r_o = 0.03$ m and $Q = 1 \times 10^{-5}$ m^3 s^{-1}.

contact angle under dynamic conditions either by theoretical estimation or by experimental measurements. This model is therefore not intended to give accurate predictions of the ligament formation radius but rather to shed some light on the mechanisms by which the processing conditions affect the melt disintegration and consequently the droplet size distribution.

The disintegration process of the melt in centrifugal atomization can be envisaged from the development of the melt flow in relation to two critical radii. The melt flow is initially a continuous thin film. At r_{c1}, the melt film breaks up into ligaments. The ligaments further break up into individual droplets at a second critical radius, defined as the droplet formation radius, r_{c2}. The three modes of atomization, namely direct droplet formation, ligament disintegration and sheet disintegration, found in centrifugal atomization can be well explained by the relationship

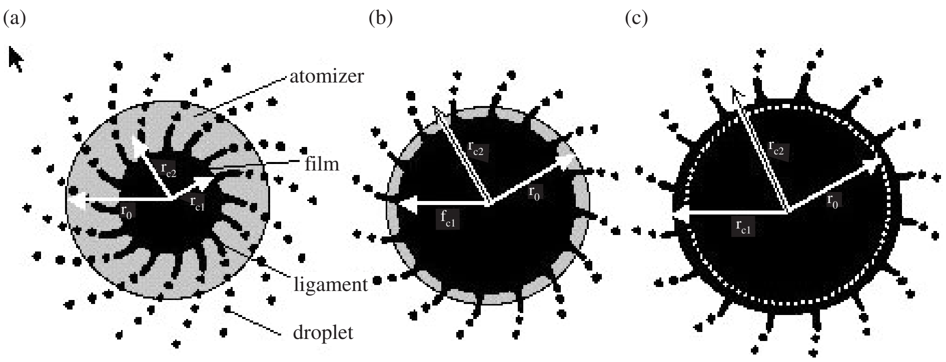

Figure 6. Schematic of the three disintegration modes: (*a*) direct droplet formation ($r_o > r_{c2}$), (*b*) ligament disintegration ($r_{c1} < r_o < r_{c2}$), and (*c*) sheet disintegration ($r_o < r_{c1}$).

between the cup radius, r_o, the ligament formation radius, r_{c1}, and the droplet formation radius, r_{c2}. The conditions $r_o > r_{c2}$, $r_{c1} < r_o < r_{c2}$ and $r_o < r_{c1}$ correspond to the melt being in droplets, ligaments and sheet at the edge of the cup and thus the respective mechanisms, as shown schematically in figure 6. In practice, two or three different modes often co-exist because of the non-steady melt flow on the cup caused by a discontinuous melt stream from the pouring nozzle [2].

In centrifugal atomization, the mean size of the atomized droplets is largely dependent upon the thickness of the film immediately prior to the disintegration. For a fully spreading melt ($r_o < r_{c1}$), the disintegration is expected to take place near the edge of the disc or cup [1]. The film thickness at the edge of the disc or cup and consequently the likely mean droplet sizes as a function of the processing condition can be predicted using the analytical model developed in part I [1]. For a non-fully spreading melt ($r_o > r_{c1}$), however, the prediction of the film thickness at the point of disintegration and consequently the likely mean droplet sizes needs the knowledge of the ligament formation radius. An understanding of the effects of the processing parameters, such as the melt flow rate, cup rotation speed and cup slope angle, on the droplet size distribution can only be achieved by combining the analytical model developed in part I [1] and the current model.

Our previous work [2] has shown that decreasing the melt flow rate and increasing the disc rotation speed generally lead to decreased sizes of the atomized droplets, which is consistent with the predictions by the analytical model for fully spreading melts [1] that the film thickness at the disc edge decreases with decreasing volume flow rate and with increasing disc rotation speed. However, there exist a minimum melt flow rate and a maximum disc rotation speed beyond which varying the flow rate or rotation speed has no effect on the droplet size distribution [2]. This is likely because decreasing the melt flow rate or increasing the disc rotation speed leads to a decreased critical contact angle for a flat disc, as shown in figures 4 and 5, and therefore a decreased ligament formation radius. When the ligament formation radius becomes smaller than the disc radius, the decrease in film thickness caused by decreasing melt flow rate or increasing disc rotation speed may be offset by the decrease in the ligament formation radius. The film thickness prior to the disintegration, and therefore the droplet sizes, may remain more or less constant. The work cited above [2] has also shown that the mean droplet size decreases with increasing cup slope angle up to a point when the other operating parameters are fixed. This is contrary to the predictions by the analytical model for fully spreading melts [1] that the film thickness at the cup edge increases with increasing cup slope angle. In fact, the cup slope angle has a marked effect on the critical contact angle, as shown in figure 3. The critical contact angle is very small on a flat disc but increases rapidly with increasing cup slope angle.

Therefore, a non-fully wetting melt on a flat disc is most likely to disintegrate well before reaching the disc edge. Increasing the cup slope angle increases the ligament formation radius and therefore may decrease the corresponding film thickness and consequently the mean droplet size. If the cup slope angle is big enough to ensure that the melt spreads fully on the cup, increasing the slope angle further has no benefits.

The present model shows that the dynamic contact angle has a significant effect on the atomization of the melt. Full wettability between the melt and the atomizing disc or cup is desirable for obtaining full spreading and thus small droplets. In practice, however, full wettability does not exist. It is difficult to ensure an extremely low dynamic contact angle, required for full spreading on a flat disc. Good spreading of the melt can be achieved more effectively by adopting an atomizing cup with an appropriate slope angle. In any case, the wetting condition may prevent the film thickness from being reduced to below a certain level. There might exist a lower limit to the primary droplet sizes obtainable in centrifugal atomization.

The present model explains well the existence of an optimum cup radius, cup slope angle, cup rotation speed and melt flow rate in centrifugal atomization. The optimum cup radius is in the vicinity of the ligament formation radius, r_{c1}. If $r_o < r_{c1}$, the greater cup radius results in a thinner melt film at the cup edge and consequently finer droplets. If $r_o > r_{c1}$, however, increasing the cup radius has little effect on the droplet sizes but increases the torque on the driving motor. The optimum cup slope angle, cup rotation speed and melt flow rate are those that make the ligament formation radius approximate the cup radius. Lower cup slope angles, lower melt flow rates or higher cup rotation speeds lead to premature disintegration and thus a low efficiency. Higher cup slope angles, higher melt flow rates or lower cup rotation speeds, however, lead to atomization in the sheet formation regime and consequently coarse particles.

4. Conclusion

A model has been developed for analysing the flow development of a non-fully spreading melt on the atomizing cup in centrifugal atomization. The model shows that the melt can disintegrate prematurely before reaching the edge of the cup when the dynamic contact angle of the melt exceeds a critical contact angle. The critical contact angle is very small for a flat disc but increases markedly with increasing slope angle of a cup. The critical contact angle also increases with increasing melt flow rate and cup rotation speed. The model explains well the phenomena observed in centrifugal atomization, including the conditions of the occurrence of the three atomization modes and the existence of an optimum melt flow rate, cup radius, cup slope angle and cup rotation speed for achieving small droplet sizes.

Acknowledgments

The author would like to thank Mr John Dunkley and Dr Jiwei Xie for some helpful discussions.

References

[1] Zhao Y Y 2004 Analysis of flow development in centrifugal atomisation part I: film thickness of a fully spreading melt *Modelling Simul. Mater. Sci. Eng.* **12** 959

[2] Xie J W, Zhao Y Y and Dunkley J J 2004 Effect of processing parameters on powder size distribution and morphology in centrifugal atomisation of tin *Powder Metall.* **47** 168–72

[3] Zhao Y Y, Dowson A L, Johnson T P, Young J M and Jacobs M H 1996 *Advances in Powder Metallurgy & Particulate Materials* vol 3, ed T M Cadle and K S Narasimhan (Princeton, NJ: Metal Powder Industries Federation) p 9.79

[4] Zhao Y Y, Dowson A L and Jacobs M H 2000 Modelling 2000 *Modelling Simul. Mater. Sci. Eng.* **8** 55
[5] Hinze J O and Milborn M 1950 *J. Appl. Mech.* **17** 145
[6] Asthana R and Sobczak N 2000 *JOM-e* **52** 1
[7] Dullien F A L 1979 *Porous Media—Fluid Transport and Pore Structure* (New York: Academic) p 8
[8] White F M 1994 *Fluid mechanics* 3rd edn (New York: McGraw-Hill) p 138
[9] Yule A J and Dunkley J J 1994 *Atomization of Melts for Powder Production and Spray Deposition* (Oxford: Clarendon)